Journal of Biomechanics 159 (2023) 111797

Contents lists available at ScienceDirect

Journal of Biomechanics

journal homepage: www.elsevier.com/locate/jbiomech

Enhanced external counterpulsation treatment regulates blood flow and wall shear stress metrics in femoral artery: An *in vivo* study in healthy subjects

Jianhang Du [a,b,*,1], Junping Peng [c,1], Xuelian Shen [d], Xiaoling Li [e], Huiling Zhong [a,b], Zhuxuan Gao [f], Muyan Chen [f], Lin Qi [f], Qilian Xie [g]

[a] *Medical Research Center, the Eighth Affiliated Hospital of Sun Yat-sen University, Shenzhen 518033, China*
[b] *National Health Commission (NHC) Key Laboratory of Assisted Circulation (Sun Yat-sen University), Guangzhou 510080, China*
[c] *Department of Radiology, The Eighth Affiliated Hospital, Sun Yat-sen University, Shenzhen 518033, China*
[d] *Department of Ultrasound, The Eighth Affiliated Hospital, Sun Yat-sen University, Shenzhen 518033, China*
[e] *Community Health Service Management Center, The Eighth Affiliated Hospital of Sun Yat-sen University, Shenzhen, China*
[f] *College of Medicine and Biological Information Engineering, Northeastern University, Shenyang 110819, China*
[g] *Department of Pediatrics, Children's Hospital of Anhui Medical University, Hefei 230051, China*

ARTICLE INFO

Keywords:
Lower-extremity artery disease
Enhanced external counterpulsation
Femoral artery
Wall shear stress

ABSTRACT

As a non-invasive assisted circulation therapy, enhanced external counterpulsation (EECP) has demonstrated potential in treatment of lower-extremity arterial disease (LEAD). However, the underlying hemodynamic mechanism remains unclear. This study aimed to conduct the first prospective investigation of the EECP-induced responses of blood flow behavior and wall shear stress (WSS) metrics in the femoral artery. Twelve healthy male volunteers were enrolled. A Doppler ultrasound-based approach was introduced for the *in vivo* determination of blood flow in the common femoral artery (CFA) and superficial femoral artery (SFA) during EECP intervention, with incremental treatment pressures ranging from 10 to 40 kPa. Three-dimensional subject-specific numerical models were developed in 6 subjects to quantitatively assess variations in WSS-derived hemodynamic metrics in the femoral bifurcation. A mesh-independence analysis was performed. Our results indicated that, compared to the pre-EECP condition, both the antegrade and retrograde blood flow volumes in the CFA and SFA were significantly augmented during EECP intervention, while the heart rate remained constant. The time average shear stress (TAWSS) over the entire femoral bifurcation increased by 32.41%, 121.30%, 178.24%, and 214.81% during EECP with treatment pressures of 10 kPa, 20 kPa, 30 kPa, and 40 kPa, respectively. The mean relative resident time (RRT) decreased by 24.53%, 61.01%, 69.81%, and 77.99%, respectively. The percentage of area with low TAWSS in the femoral artery dropped to nearly zero during EECP with a treatment pressure greater than or equal to 30 kPa. We suggest that EECP is an effective and non-invasive approach for regulating blood flow and WSS in lower extremity arteries.

1. Introduction

Lower-extremity arterial disease (LEAD) is a typical manifestation of ischemic vascular disease related to chronic arterial occlusion and diabetes mellitus, and has shown increased global incidence in recent decades (Nativel et al., 2018; Chun et al., 2019). LEAD can cause severe clinical outcomes, with an increased risk of major cardiovascular events and cardiovascular mortality, and is a major cause of amputation and disability (Marso and Hiatt, 2006; Nativel et al., 2018).

LEAD is a chronic disease resulting from partial or complete obstruction of one or more lower-limb arteries (Aboyans et al., 2018). In recent decades, rehabilitation procedures based on supervised active or passive exercise have been recommended as therapy or first-line therapy for treatment of LEAD (Hamburg and Balady, 2011; Buschmann et al., Adams et al., 2021). Clinical benefits include hemodynamics, walking ability, cardiorespiratory fitness, and pain-free status (Parmenter et al.,

* Corresponding author at: 3025 Shennan Road, Shenzhen 518033, Guangdong Province, China.
E-mail address: dujh8@mail.sysu.edu.cn (J. Du).
[1] These authors have contributed equally to this work and share first authorship.

https://doi.org/10.1016/j.jbiomech.2023.111797
Received 28 February 2023; Received in revised form 25 July 2023; Accepted 5 September 2023
Available online 6 September 2023

2015). Exercise regulates vascular wall shear stress (WSS) and, in turn, improves endothelial function, which is considered to be an underlying mechanism (Werner et al., 2007; Adams et al., 2021). Compared with active exercise, passive exercise is safer, especially for patients with severe comorbidities who are unsuitable for long and intense training intervals. Enhanced external counterpulsation (EECP), as a typical passive exercise and a U.S. Food and Drug Administration (FDA)-approved non-invasive assisted-circulation technique, has exhibited hemodynamic benefits in multiple organ systems (Michaels et al., 2002; Taguchi et al., 2004; Lin et al., 2012) and vascular protective benefits (Nichols et al., 2006; Zhang et al., 2007). EECP therapy is recommended as a clinical therapeutic option for treatment of ischemic cardiovascular and cerebrovascular diseases (Tian et al., 2021).

The EECP technique, which was originally derived from our laboratory, involves application of three sets of pneumatic cuffs wrapped around the calves, lower thighs, and upper thighs of the patient, with sequential inflations and deflations synchronized with electrocardiograms (Zheng et al., 1984). Diastolic augmentation of perfusion pressure and retrograde blood flow in the aorta is achieved during EECP, as well as an increase in venous return and cardiac output (Michaels et al., 2002). LEAD was once considered a relative contraindication to EECP therapy due to potential safety concerns. However, further studies based on clinical trials have confirmed the efficacy and safety of EECP treatment in patients with LEAD, and especially diabetic foot, in the absence of leg ulcers, abdominal aortic aneurysms, and deep vein thrombosis (DVT). Thakkar et al. (2010) reported a sustained improvement in quality of life in a two-year follow-up of patients with LEAD who received EECP treatment; the adverse event rates related to skin ulceration or any limb outcome did not increase significantly. Braith et al. (2010) reported that a standard 35-h EECP treatment could lead to a 30% increase in femoral artery flow-mediated dilation (FMD) in patients with chronic angina. Several studies have confirmed the beneficial effects of long-term EECP treatment in the management of diabetes, including marked improvements in glycemic and resistance artery function of the limbs (Martin et al., 2012; Martin and Braith, 2012) and decreased levels of advanced glycation end-products and proinflammatory cytokines (Sardina et al., 2016).

However, the hemodynamic mechanisms underlying the clinical benefits of EECP in patients with LEAD remain unclear. As the hips and lower limbs of patients are tightly wrapped and covered with pneumatic cuffs, and EECP stimulus causes severe vibration, detection of blood flow in lower-extremity arteries during EECP intervention remains a technical challenge for *in vivo* and *in vitro* approaches. Gurovich and Braith. (2013) reported Doppler ultrasonography of blood flow in the common femoral arteries (CFA) of young and healthy male subjects during EECP with a 30-kPa treatment pressure. However, their results seem physiologically unreasonable; the antegrade flow rapidly dropped to zero before inflation of the cuffs was triggered, and the flow velocity remained at zero in almost half of the cardiac cycle. To the best of our knowledge, no study has reported the influence of EECP on WSS distribution in lower-extremity arteries, considering that it is accepted that WSS plays a crucial role in maintaining vascular physiological functions and atherosclerosis initiation (Samady et al., 2011).

A prospective investigation of variations in blood flow behavior and WSS metrics in the femoral artery before (resting in supine position with cuff pressure = 0 kPa) and during EECP intervention was conducted in this study, with incremental treatment pressures ranging from 10 to 40 kPa. A novel Doppler ultrasound-based approach was introduced for *in vivo* measurement of blood flow in the CFA and superficial femoral artery (SFA) during EECP. Subject-specific computational fluid dynamics (CFD) models were developed to quantitatively assess WSS and commonly used magnitude-based WSS-derived metrics including time average wall shear stress (TAWSS), oscillatory shear index (OSI), relative resident time (RRT), wall shear stress gradient (WSSG), and transverse wall shear stress (transWSS). This study may play a vital role in translation of EECP treatment for patients with LEAD.

2. Methods

2.1. Subjects and medical image acquisition

Twelve young and healthy male volunteers were enrolled in the study (27.7 ± 7.2 years of age, 171.4 ± 5 cm in height, 55.4 ± 2.9 kg in weight). All participants claimed no tobacco smoking habits and showed no history of cardiovascular disease, hypertension, hyperlipidemia, or hyperglycemia according to their latest medical examination reports. Color Doppler ultrasonic scans were performed to ensure the absence of structural lesions in the femoral or tibial arteries. Written informed consent was obtained from all participants before the experiment. This study was approved by the local medical ethics committee of the Eighth Affiliated Hospital of the Sun Yat-sen University (SYSU).

All subjects underwent magnetic resonance imaging (MRI) scans of the femoral artery using a 3.0 T MRI device (Siemens Electric Company, MAGNETOM Prisma) equipped with a high-frequency 18-channel body coil. MRI-based geometry reconstruction was performed using MIMICS 17.0 (Materialise NV, Leuven, Belgium) for the subsequent numerical analysis.

2.2. EECP intervention protocol and color Doppler ultrasound measurement

All subjects received a single session of EECP treatment for approximately 30 min, with incremental treatment pressures of 10 kPa, 20 kPa, 30 kPa, and 40 kPa. The Doppler spectrum of blood flow velocity was measured in the right femoral artery before and during EECP. Tobacco, alcohol, and caffeine consumption were restricted for at least 24 h before measurement.

A Doppler ultrasound-based approach was proposed in this study for *in vivo* detection of blood flow in the femoral artery under an EECP stimulus, and involved several key points. (I) A high-resolution ultrasound system was used. (II) A specifically designed calf and upper thigh cuff with a sufficiently large gap in the lower side of the groin was used to guarantee sufficient space for the ultrasound device probe. (III) A specifically designed bandage wrapped around the ankles was used to restrict movement of the limbs and reduce vibration. (IV) Doppler flow velocity spectrum examinations were serially performed in the right CFA and right SFA, 2–3 cm proximal to the femoral artery bifurcation. When the treatment pressure changes, EECP intervention should continue for at least 3 min before measurement, and the finger pulse signal shown on the EECP device monitor should exhibit stable waveforms in continuous cardiac cycles to guarantee that the interventions are sufficient and the measurement results are reliable. However, our blood flow detection method was not isochronous in CFA and DFA. There was a time lag of approximately 20–30 s.

A color Doppler ultrasound system (EPIQ7C, Philip Com, Netherlands) equipped with a 9–11 MHz multifrequency high-resolution linear probe was used. All measurements were performed in a clinical ultrasound room. A portable EECP device (P-ECP/TM, Chongqing PSK-Health Sci-Tech Development Co., Ltd.) was used instead of the normal EECP bed to ensure that it could be conveniently moved to the ultrasound room.

2.3. Blood flow waveform extraction

The blood flow rates in one cardiac cycle as shown in Fig. 1 were calculated based on the mean blood flow velocity waveforms and vascular diameters extracted from the ultrasound images. The vascular diameter was assumed to be constant over the cardiac cycle, calculated as (Tian et al., 2021)

$$mean\ \ diameter = \left(\frac{1}{3} \times systolic\ \ diameter\right) + \left(\frac{2}{3} \times diatolic\ \ diameter\right) \quad (1)$$

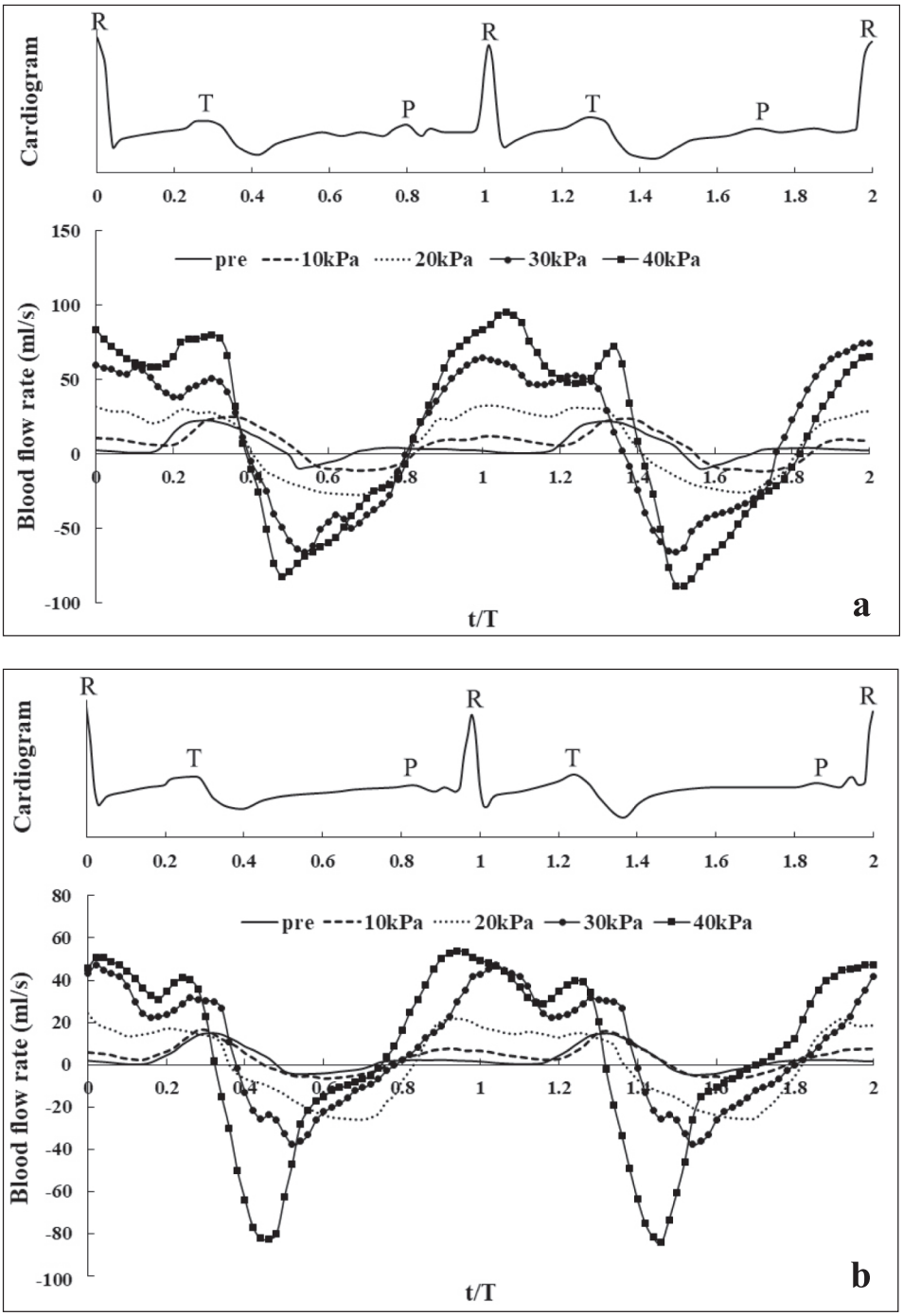

Fig. 1. Blood flow-rate curves in two continuous cardiac cycles before and during EECP intervention with incremental cuff pressure: (a) CFA; (b) SFA.

2.4. Numerical approach and boundary conditions

Subject-specific numerical simulations were performed to quantitatively assess the variations in WSS and WSS-derived hemodynamic factors in the femoral artery before and during EECP. Development of the numerical model and the subsequent post-processing are time-consuming. Blood flow patterns in the CFA and SFA with EECP intervention exhibited similar variation characteristics among the subjects. Thus, only six of the 12 subjects were selected for further numerical analysis in the current study.

The blood fluid was assumed to be impressible and isoviscous (Newtonian type $\mu = 0.039$ Pa·s). Thus, the governing equations for the transportation of blood flow in arteries were continuity and momentum equations. The original geometry consisted of four boundaries: an inlet in the CFA, two outlets in the SFA and DFA, and a wall. Blood flow rate curves (Fig. 1) were set in the CFA and SFA as the inflow and outflow boundary conditions, respectively. To guarantee fully developed velocity profiles, extensions of both the inlet and outlet boundaries at the SFA were performed outward along their normal directions for lengths five times their average radius (Tian et al., 2021). The opening condition was set for the outlet boundary of the DFA. A previous study confirmed that wall motion does not have a significant influence on the global fluid dynamic characteristics of the femoral bifurcation (Kim et al., 2008). Thus, the elasticity of the vessel wall was ignored in this study, and a no-slip boundary condition was used at the wall.

2.5. Mesh generation and mesh-independence analysis

The computational mesh for hemodynamic analysis was generated using the ICEM 17.0 package (Ansys Inc., Canonsburg, PA, USA). The geometry was meshed using tetrahedral cells in the core region. In the near-wall region, with a high variable gradient, ten inflation layers were generated to improve the solution accuracy. A mesh-independence study was performed on a randomly selected research subject. The mesh used in the independence study contained incremental quantities of 460,000, 910,000, 1,610,000, and 3,420,000 elements. The computational results based on a mesh quantity of 3,420,000 were used as the ground truth data. TAWSS results based on different mesh sizes were extracted from three cross-sections in the CFA, SFA, and DFA, approximately 1.0 cm proximal to the bifurcation apex. Compared to the ground truth data, relative errors were calculated at ten selected points uniformly distributed at the walls of the cross-sections. Table 1 presents the results of the mesh-independence study. The optimized mesh contained 910,000 elements, producing reliable results (mean errors $\leq$ 5%) and an acceptable computational burden.

2.6. Solution methods

The governing equations were discretized using a finite-volume method (FVM) based on the CFX 18.2 package (Ansys Inc., Canonsburg, PA, USA). Numerical solutions were obtained; the root mean squares (RMS) of the mass and momentum residuals were$<10^{-5}$. Unknowns were resolved using this configuration for three cardiac cycles. The results of the first and second cardiac cycles were used to initialize the computational domain; the results presented in the following sections were collected from the third cardiac cycle.

2.7. Statistical analysis

One-way repeated measures analysis of variance (ANOVA) was used to test the influence of EECP intervention on blood flow volume and WSS-derived metrics. The Bonferroni correction was performed for multiple comparisons. Data analysis was performed using SPSS statistical software version 25.0 (IBM SPSS Statistics, Armonk, NY, USA). Data are presented as the mean $\pm$ SD. A statistical value of $p < 0.05$ was considered statistically significant.

3. Results and discussion

3.1. Effects of EECP on blood flow behavior

EECP intervention caused an apparent alteration of the blood flow patterns in both the CFA and SFA, especially when the treatment pressure was greater than or equal to 20 kPa (Fig. 1). The sequential distal-to-proximal inflations of the three sets of pneumatic cuffs, which were triggered by the T wave on the ECG signal, led to a rapid turn of the antegrade blood flow in the systole and significant augmentation of the retrograde blood flow. The pneumatic cuffs deflated synchronously during late diastole, which led to a rapid increase in antegrade blood flow. The blood flow volume over cardiac cycles may be altered by EECP intervention. Fig. 2 shows the statistics of the antegrade and retrograde blood flow volumes over one cardiac cycle before and during EECP intervention with incremental treatment pressures. The blood flow volume was calculated using the integral of the blood flow rate over the cardiac cycle.

Our results indicated that the overall blood flow volumes before EECP in the CFA and SFA were 354.31 $\pm$ 93.75 ml/min and 137.17 $\pm$ 38.55 ml/min, respectively, consistent with the range of reported measured results (Liang, 2020). Compared with the pre-EECP condition, EECP with treatment pressures of 10 kPa, 20 kPa, 30 kPa, and 40 kPa increased 34.79%, 135.85%, 287.11%, and 394.35% of the antegrade blood flow volume in the CFA, and 126.32%, 578.92%, 1119.33%, and 1375.18% of the retrograde blood flow volume, respectively. All of the differences were statistically significant ($p < 0.05$). In the SFA, EECP led to 59.82%, 234.57%, 367.96%, and 477.82% increases in antegrade blood flow volume, and 107.65%, 476.36%, 798.52%, and 1183.26% increases in retrograde blood flow volume, respectively. The differences were statistically significant when the cuff pressure was greater than or equal to 20 kPa. Both antegrade and retrograde blood flow volumes over one cardiac cycle were positively proportional to treatment pressure.

Heart rates (HR) of the subjects pre-EECP and during EECP with treatment pressures of 10 kPa, 20 kPa, 30 kPa, and 40 kPa were 70.73 $\pm$ 9.87, 72.64 $\pm$ 7.83, 72.77 $\pm$ 8.91, 70.32 $\pm$ 6.05, and 70.7 $\pm$ 6.34,

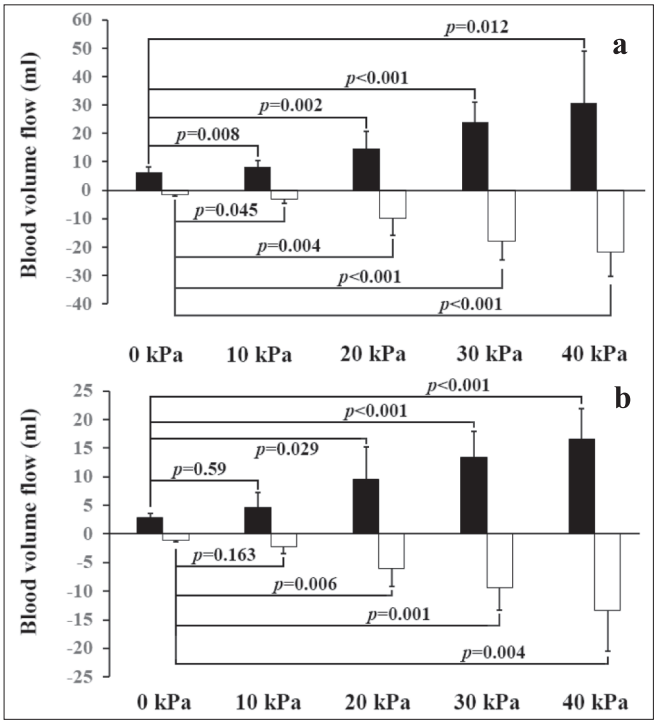

Fig. 2. Blood volume flow variations before and during EECP intervention: (a) CFA; (b) SFA. Closed boxes (■) and open boxes (□) represent antegrade flow and retrograde flow, respectively, over one cardiac cycle.

Table 1
The results of the mesh-independence study.

	Before EECP (Rest)			During EECP		
Mesh quantity	460,000	910,000	1,610,000	460,000	910,000	1,610,000
Mean Errors (%)						
CFA	5.34 $\pm$ 2.02	1.86 $\pm$ 1.47	0.5 $\pm$ 0.34	10.94 $\pm$ 7.10	4.76 $\pm$ 2.93	3.39 $\pm$ 1.95
SFA	3.41 $\pm$ 1.04	1.15 $\pm$ 0.85	0.78 $\pm$ 0.49	6.69 $\pm$ 2.96	3.29 $\pm$ 2.29	2.56 $\pm$ 1.27
DFA	8.88 $\pm$ 2.57	1.82 $\pm$ 1.59	1.19 $\pm$ 0.81	13.62 $\pm$ 2.42	2.21 $\pm$ 2.20	1.07 $\pm$ 0.72

Note that the data shown in the table represents the relative error between the computational results and the ground truth data. The EECP treatment pressure used in the mesh-independence study was 30 kPa.

respectively. Compared with the pre-EECP condition, EECP intervention led to a plateau in the HR, even with higher treatment pressures of 30 kPa and 40 kPa. Similar results were confirmed in clinical trials of patients with cardiovascular disease (Taguchi et al., 2004; Campbell et al., 2008).

3.2. Influence of EECP on WSS and WSS-derived metrics

Wall shear stress (WSS) is defined as the tangential frictional force exerted on the endothelial surface by flowing blood, and is largely dependent on the specific geometric characteristics of the vessel. It is generally accepted that low and oscillatory WSS (e.g., at arterial bifurcations or distal segments of plaques) outside the physiological range plays a crucial role in generation and progression of atherosclerotic lesions (Samady et al., 2011; De Wilde et al., 2016).

The temporary WSS distributions in the femoral bifurcation in one cardiac cycle before and during EECP with incremental treatment pressures are shown in Fig. 3, involving four spatial points located at different sites: the proximal CFA, proximal SFA, proximal DFA, and apex. EECP intervention induced an apparent alteration in the WSS pattern as well as an increase in WSS magnitude, especially when the treatment pressure was greater than or equal to 20 kPa. In this subject, the peak WSS in the cardiac cycle was 88.56 Pa, which occurred at the apex with an EECP treatment pressure of 40 kPa.

Considering that WSS is a hemodynamic parameter that is continuous and oscillatory, WSS-derived hemodynamic metrics have been proposed by different research groups to quantitatively assess the magnitude and fluctuation of WSS over the cardiac cycle, for example, TAWSS, OSI, RRT, AWSSG, and transWSS. In recent decades, many studies have demonstrated a possible correlation between atherosclerotic lesions and WSS metrics (Rikhtegar et al., 2012; Colombo et al., 2022). In an intensive study that linked WSS metrics to atherosclerosis development in a murine carotid bifurcation model, De Wilde et al. (2016) confirmed that the strongest spatial correlation between hemodynamics and atherosclerosis development was observed for RRT and TAWSS. The general expressions for these WSS metrics are presented as follows.

$$\mathrm{TAWSS} = \frac{1}{T}\int_0^T \left|\vec{\tau}_w\right| dt \tag{1}$$

$$\mathrm{WSSG} = \sqrt{\left(\left|\frac{\partial \vec{\tau}_w}{\partial x}\right|\right)^2 + \left(\left|\frac{\partial \vec{\tau}_w}{\partial y}\right|\right)^2 + \left(\left|\frac{\partial \vec{\tau}_w}{\partial z}\right|\right)^2} \tag{2}$$

$$\mathrm{AWSSG} = \frac{1}{T}\int_0^T WSSG dt \tag{3}$$

$$\mathrm{OSI} = \frac{1}{2}\left(1 - \frac{\left|\int_0^T \vec{\tau}_w dt\right|}{\int_0^T \left|\vec{\tau}_w\right| dt}\right) \tag{4}$$

$$\mathrm{RRT} = \frac{1}{(1 - 2\cdot \mathrm{OSI})\cdot \mathrm{TAWSS}} \tag{5}$$

$$\mathrm{transWSS} = \frac{1}{T}\int_0^T \left|\vec{\tau}_w \cdot \left(\vec{n} \times \frac{\int_0^T \vec{\tau}_w dt}{\left|\int_0^T \vec{\tau}_w dt\right|}\right)\right| dt \tag{5}$$

where $\left|\vec{\tau}_w\right|$ is the magnitude of the instantaneous WSS vector $\vec{\tau}_w$, and T is the duration of one cardiac cycle. $\vec{n}$ represents normal to the vascular surface.

The overall effects of EECP with incremental treatment pressures on WSS metrics are shown and graphically compared in Fig. 4. As it was suggested that the correlation between atherosclerotic lesions and WSS metrics was most apparent when assessed at the level of the entire bifurcation (De Wilde et al., 2016), area-averaged values of the metrics

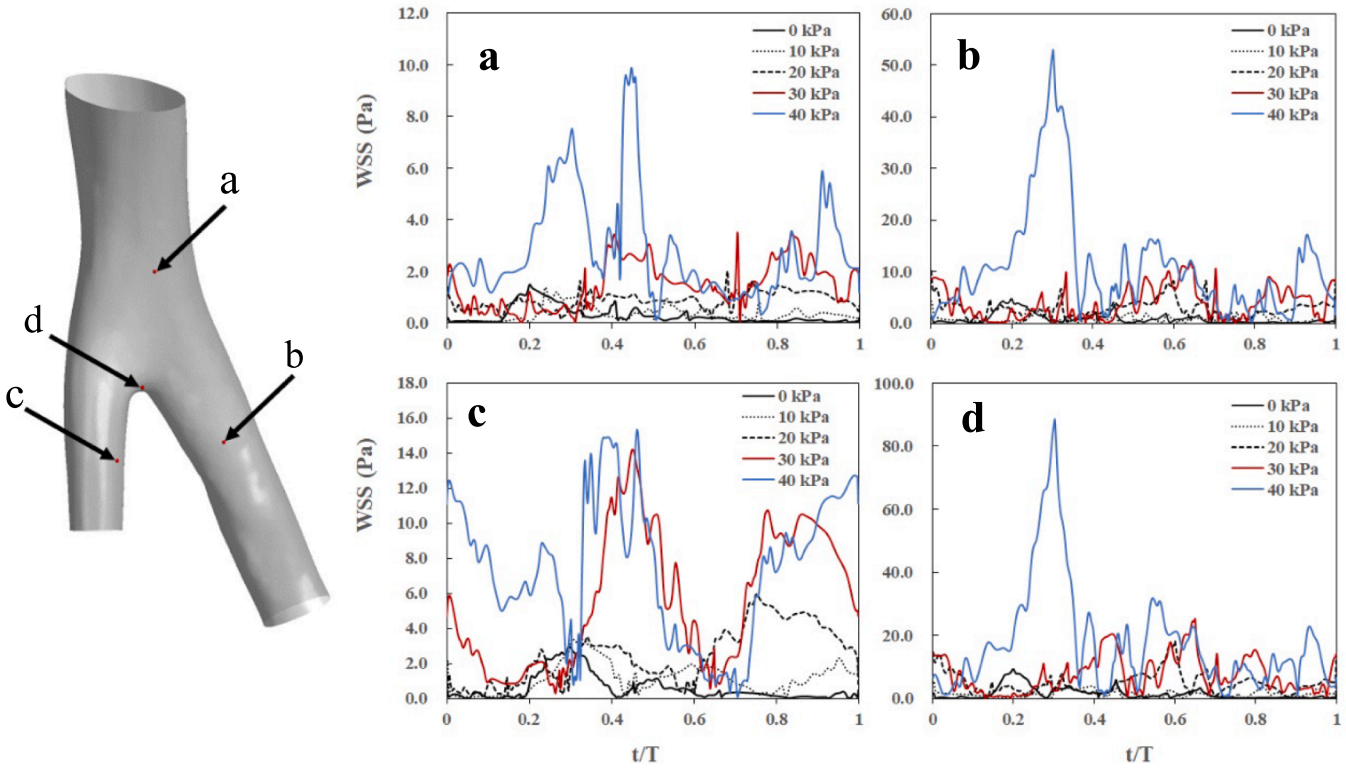

Fig. 3. WSS distributions in a cardiac cycle before and during EECP intervention in the femoral bifurcation: (a) proximal CFA; (b) proximal SFA; (c) proximal DFA; (d) the apex.

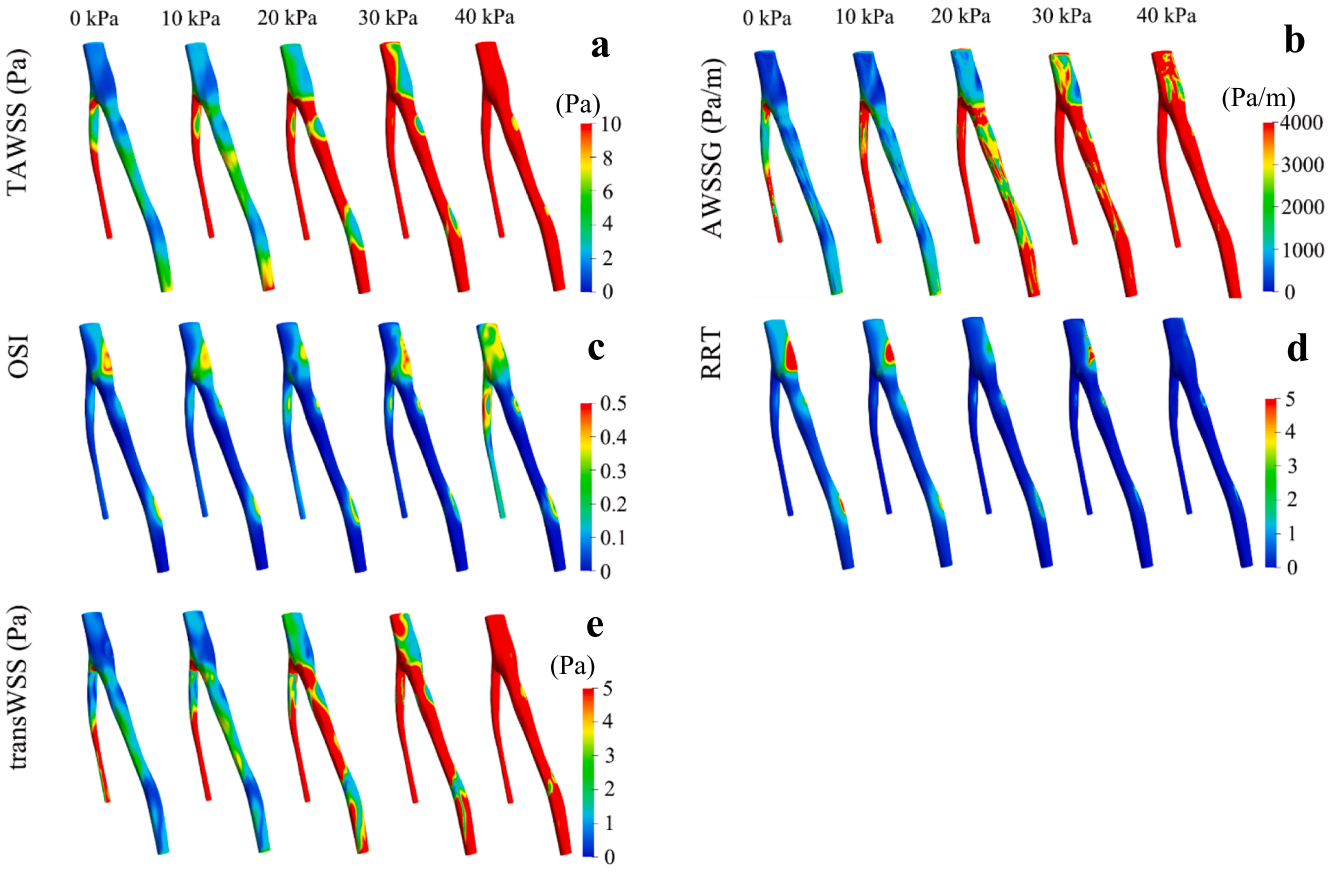

Fig. 4. Distributions of WSS metrics over one cardiac cycle before and during EECP with incremental treatment pressures of 10 kPa, 20 kPa, 30 kPa, and 40 kPa: (a) TAWSS; (b) AWSSG; (4) OSI; (d) RRT; (e) transWSS.

were calculated throughout the femoral bifurcation geometry.

TAWSS is proposed to represent the WSS magnitude averaged over the cardiac cycle and was confirmed to be highly sensitive in predicting plaque locations (Rikhtegar et al., 2012). Samady et al (2011) suggested that an atherosclerotic plaque area increase was associated with low-TAWSS (<1.0 Pa) arterial segments, and a decrease in plaque area was correlated with intermediate- (≥1.0 and < 2.5 Pa) and high-TAWSS (≥2.5 Pa) arterial segments. Our results showed that EECP intervention can efficiently augment the overall TAWSS level. A positive correlation was observed between the TAWSS and ECCP treatment pressure. Compared to the pre-EECP condition, the mean TAWSS increased by 32.41%, 121.30%, 178.24%, and 214.81% during EECP with treatment pressures of 10 kPa, 20 kPa, 30 kPa, and 40 kPa, respectively. Our results showed that EECP intervention led to an apparent decrease in the percentage of low-TAWSS area (see Fig. 5). When the treatment pressure was greater than or equal to 30 kPa, the percentage of low-TAWSS area in the femoral bifurcation was close to 0.

Fig. 4b shows the RTT contours before and during EECP. RRT is a

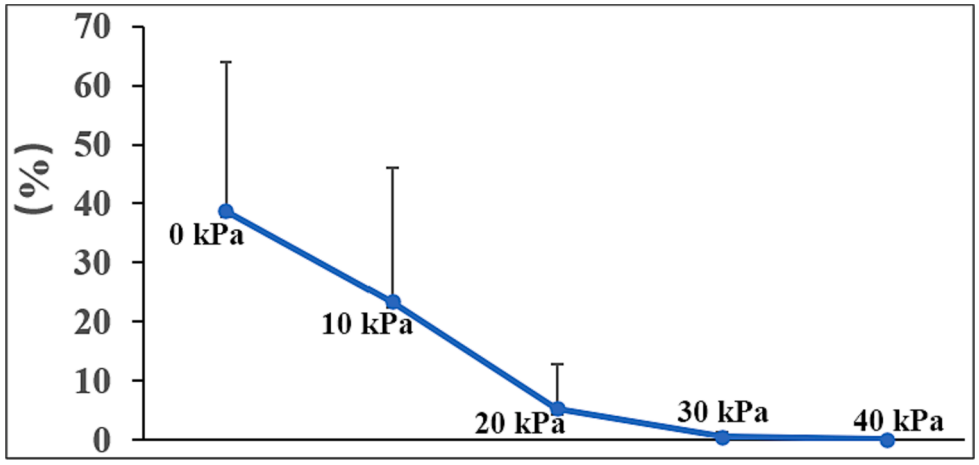

Fig. 5. Percentage variation in low-TAWSS area before and during EECP. Statistics were calculated throughout the femoral bifurcation model; six subjects were involved.

WSS-derived metric introduced to quantify the residence time of molecules in arterial segments. Previous studies have demonstrated a positive correlation between the sites of plaque initiation and high-level RRT (Hoi et al., 2011; Chen et al., 2017). Our study showed that EECP intervention efficiently reduced the RRT levels over the femoral bifurcation. A negative correlation was observed between RRT and ECCP cuff pressure. Compared to the pre-EECP condition, the mean RRT decreased by 24.53%, 61.01%, 69.81%, and 77.99% at treatment pressures of 10 kPa, 20 kPa, 30 kPa, and 40 kPa, respectively. However, these differences were not statistically significant.

OSI is a WSS-derived metric proposed to quantify the temporal oscillation of the WSS. The results of this study indicate that EECP intervention leads to a plateau or slight decrease in the OSI level over the femoral bifurcation. In some cases, the OSI in the proximal DFA showed an apparent increase during EECP with a treatment pressure of 40 kPa (Fig. 3c).

Fig. 4b shows the AWSSG contours in the femoral bifurcation before and during EECP with incremental treatment pressures. AWSSG represents the WSSG magnitude averaged over one cardiac cycle; WSSG was proposed to quantify the spatial oscillation of the WSS. Some studies have demonstrated that high WSSG levels are correlated with neointimal hyperplasia (Buchanan et al., 1999). A positive correlation was observed between the AWSSG level and EECP treatment pressure. Compared with the pre-EECP condition, the area-averaged AWSSG increased by 20.33%, 120.11%, 193.85%, and 233.0% during EECP at treatment pressures of 10 kPa, 20 kPa, 30 kPa, and 40 kPa, respectively.

Fig. 4e shows the transWSS contours in the femoral bifurcation before and during EECP intervention to capture the multidirectional characteristics of the WSS (Mohamied et al., 2015). Our results indicated a positive correlation between transWSS levels and ECCP treatment pressure. Compared with the pre-EECP condition, the area-averaged transWSS increased by 23.86%, 134.09%, 197.73%, and 279.54% at treatment pressures of 10 kPa, 20 kPa, 30 kPa, and 40 kPa, respectively.

3.3. Limitations

The current study has some limitations. Firstly, only young and healthy male subjects were involved in this study based on similar considerations of Gurovich and Braith (2013), and the sample size was relatively low. Diabetic foot patients of Wagner grade 0 to grade 1 have been considered to be recruited in further work. Secondary, the CFD analysis was performed only on half of the subjects, considering that numerical simulations and subsequent post-processing were rather time- and effort- consuming and he exploratory nature of this study. Eventually, the elasticity of the vessel wall as well as the non-Newtonian blood rheological model was ignored in our current CFD simulations.

4. Conclusion

To the best of our knowledge, this is the first prospective investigation of the influence of EECP treatment on WSS-derived hemodynamic metrics in the femoral bifurcation. Our study revealed that EECP intervention significantly augmented antegrade blood volume flow and TAWSS level in femoral arteries, with an apparent decrease in RRT and the percentage of area with low TAWSS. EECP does not increase HR as passive physical exercise does. These hemodynamic benefits suggest that EECP may be an effective and non-invasive approach for regulating blood flow and WSS in lower limbs. However, it will need a further long-term and follow-up control study to confirm the proper benefits and safety of EECP treatment in LEAD patients. Finally, although a positive correlation was observed between hemodynamic benefits and EECP cuff pressure, a treatment pressure greater than or equal to 30 kPa is not recommended due to a higher risk of discomfort and hypertension-related adverse effects such as skin abrasions (Lin et al., 2012).

CRediT authorship contribution statement

Jianhang Du: Writing – review & editing, Writing – original draft, Validation, Software, Methodology, Investigation, Funding acquisition, Conceptualization. **Junping Peng:** Writing – review & editing, Visualization, Software, Methodology, Investigation. **Xuelian Shen:** Writing – review & editing, Investigation, Data curation. **Xiaoling Li:** Investigation, Formal analysis, Data curation. **Huiling Zhong:** Visualization, Software, Data curation. **Zhuxuan Gao:** Validation, Investigation. **Muyan Chen:** Validation, Investigation. **Lin Qi:** Writing – review & editing, Supervision. **Qilian Xie:** Writing – review & editing, Supervision, Funding acquisition.

Declaration of Competing Interest

The authors declare that they have no known competing financial interests or personal relationships that could have appeared to influence the work reported in this paper.

Acknowledgements

This work is supported by National Key R&D Program of the Ministry of Science and Technology of China (Grant No. 2020YFC2004403), Science and Technology Planning Project of Shenzhen Municipality (Grant No. JCY20180306174831458 and GJHZ20200731095008026), Public Health Key Project of Futian District of Shenzhen (FTWS2021001).

References

Aboyans, V., Ricco, J.B., Bartelink, M.E.L., et al., 2018. 2017 ESC guidelines on the diagnosis and treatment of peripheral arterial diseases, in collaboration with the European Society for Vascular Surgery (ESVS). Eur. Heart J. 39, 763–816.
Adams, J.A., Uryash, A., Lopez, J.R., et al., 2021. The Endothelium as a Therapeutic Target in Diabetes: A Narrative Review and Perspective. Front. Physiol. 12, 638491.
Braith, R.W., Conti, C.R., Nichols, W.W., et al., 2010. Enhanced external counterpulsation improves peripheral artery flow-mediated dilation in patients with chronic angina: a randomized sham-controlled study. Circulation 16 (122), 1612–1620.
Buchanan, J.R., Kleinstreuer, C., Truskey, G.A., Lei, M., et al., 1999. Relation between non-uniform hemodynamics and sites of altered permeability and lesion growth at the rabbit aorto-celiac junction. Atherosclerosis 1 (143), 27–40.
Campbell, A.R., Satran, D., Zenovich, A.G., et al., 2008. Enhanced external counterpulsation improves systolic blood pressure in patients with refractory angina. Am. Heart J. 6 (156), 1217–1222.
Chen, Z., Yu, H., Shi, Y., et al., 2017. Vascular Remodelling Relates to an Elevated Oscillatory Shear Index and Relative Residence Time in Spontaneously Hypertensive Rats. Sci. Rep. 1 (7), 2007.
Chun, D.I., Kim, S., Kim, J., et al., 2019. Epidemiology and Burden of Diabetic Foot Ulcer and Peripheral Arterial Disease in Korea. J. Clin. Med. 5 (8), 748–753.
Colombo, M., Corti, A., Gallo, D., et al., 2022. Superficial femoral artery stenting: Impact of stent design and overlapping on the local hemodynamics. Comput. Biol. Med. 143, 105248.
De Wilde, D., Trachet, B., De Meyer, G.R., et al., 2016. Shear Stress Metrics and Their Relation to Atherosclerosis: An In Vivo Follow-up Study in Atherosclerotic Mice. Ann. Biomed. Eng. 44, 2327–2338.
Gurovich, A.N., Braith, R.W., 2013. Enhanced external counterpulsation creates acute blood flow patterns responsible for improved flow-mediated dilation in humans. Hypertens. Res. 4 (36), 297–305.
Hamburg, N.M., Balady, G.J., 2011. Exercise rehabilitation in peripheral artery disease: functional impact and mechanisms of benefits. Circulation. 1 (123), 87–97.
Hoi, Y., Zhou, Y.Q., Zhang, X., et al., 2011. Correlation between local hemodynamics and lesion distribution in a novel aortic regurgitation murine model of atherosclerosis. Ann. Biomed. Eng. 5 (39), 1414–11222.
Kim, Y.H., Kim, J.E., Ito, Y., et al., 2008. Hemodynamic analysis of a compliant femoral artery bifurcation model using a fluid structure interaction framework. Ann. Biomed. Eng. 11 (36), 1753–1763.
Liang, H.L., 2020. Doppler Flow Measurement of Lower Extremity Arteries Adjusted by Pulsatility Index. AJR. Am. J. Roentgenol. 1 (214), 10–17.
Lin, W., Xiong, L., Han, J., et al., 2012. External counterpulsation augments blood pressure and cerebral flow velocities in ischemic stroke patients with cerebral intracranial large artery occlusive disease. Stroke. 11 (43), 3007–3011.
Marso, S.P., Hiatt, W.R., 2006. Peripheral arterial disease in patients with diabetes. J. Am. Coll. Cardiol. 5 (47), 921–929.
Martin, J.S., Beck, D.T., Aranda Jr., J.M., Braith, R.W., et al., 2012. Enhanced external counterpulsation improves peripheral artery function and glucose tolerance in subjects with abnormal glucose tolerance. J. Appl. Physiol. 5 (112), 868–876.

Martin, J.S., Braith, R.W., 2012. Anti-inflammatory effects of enhanced external counterpulsation in subjects with abnormal glucose tolerance. Appl. Physiol. Nutr. Metab. 6 (37), 1251–1255.
Michaels, A.D., Accad, M., Ports, T.A., Grossman, W., 2002. Left ventricular systolic unloading and augmentation of intracoronary pressure and Doppler flow during enhanced external counterpulsation. Circulation. 10 (106), 1237–1242.
Mohamied, Y., Rowland, E.M., Bailey, E.L., et al., 2015. Change of Direction in the Biomechanics of Atherosclerosis. Ann. Biomed. Eng. 43, 16–25.
Nativel, M., Potier, L., Alexandre, L., et al., 2018. Lower extremity arterial disease in patients with diabetes: a contemporary narrative review. Cardiovasc. Diabetol. 1 (17), 138.
Nichols, W.W., Estrada, J.C., Braith, R.W., et al., 2006. Enhanced external counterpulsation treatment improves arterial wall properties and wave reflection characteristics in patients with refractory angina. J. Am. Coll. Cardiol. 6 (48), 1208–1214.
Parmenter, B.J., Dieberg, G., Smart, N.A., 2015. Exercise training for management of peripheral arterial disease: a systematic review and meta-analysis. Sports Med. 2 (45), 231–244.
Rikhtegar, F., Knight, J.A., Olgac, U., et al., 2012. Choosing the optimal wall shear parameter for the prediction of plaque location-A patient-specific computational study in human left coronary arteries. Atherosclerosis 2 (221), 432–437.
Samady, H., Eshtehardi, P., Mcdaniel, M.C., et al., 2011. Coronary artery wall shear stress is associated with progression and transformation of atherosclerotic plaque and arterial remodeling in patients with coronary artery disease. Circulation 124, 779–788.
Sardina, P.D., Martin, J.S., Dzieza, W.K., Braith, R.W., et al., 2016. Enhanced external counterpulsation (EECP) decreases advanced glycation end products and proinflammatory cytokines in patients with non-insulin-dependent type II diabetes mellitus for up to 6 months following treatment. Acta Diabetol. 5 (53), 753–760.
Taguchi, I., Ogawa, K., Kanaya, T., et al., 2004. Effects of enhanced external counterpulsation on hemodynamics and its mechanism. Circ. J. 11 (68), 1030–1034.
Thakkar, B.V., Hirsch, A.T., Satran, D., et al., 2010. The efficacy and safety of enhanced external counterpulsation in patients with peripheral arterial disease. Vasc. Med. 1 (15), 15–20.
Tian, S., Pan, W., Peng, J., et al., 2021. Hemodynamic Responses in Carotid Bifurcation Induced by Enhanced External Counterpulsation Stimulation in Healthy Controls and Patients With Neurological Disorders. Front. Physiol. 717080.
Zhang, Y., He, X., Chen, X., et al., 2007. Enhanced external counterpulsation inhibits intimal hyperplasia by modifying shear stress-responsive gene expression in hypercholesterolemic pigs. Circulation. 5 (116), 526–534.
Zheng, Z.S., Yu, L.Q., Cai, S.R., et al., 1984. New sequential external counterpulsation for the treatment of acute myocardial infarction. Artif. Organs. 4 (8), 470–477.